

## RESEARCH ARTICLES

# Rha1, an Arabidopsis Rab5 Homolog, Plays a Critical Role in the Vacuolar Trafficking of Soluble Cargo Proteins

Eun Ju Sohn,<sup>a,b</sup> Eol Sun Kim,<sup>a</sup> Min Zhao,<sup>c</sup> Soo Jin Kim,<sup>a</sup> Hyeran Kim,<sup>d</sup> Yong-Woo Kim,<sup>d</sup> Yong Jik Lee,<sup>d</sup> Stefan Hillmer,<sup>e</sup> Uik Sohn,<sup>b</sup> Liwen Jiang,<sup>c</sup> and Inhwan Hwang<sup>a,d,1</sup>

<sup>a</sup> Center for Plant Intracellular Trafficking, Pohang University of Science and Technology, Pohang 790-784, Korea

<sup>b</sup> Department of Genetic Engineering, Kyungpook National University, Daegu 702-701, Korea

<sup>c</sup> Department of Biology, The Chinese University of Hong Kong, Shatin, New Territories, Hong Kong, China

<sup>d</sup> Division of Molecular and Life Sciences, Pohang University of Science and Technology, Pohang 790-784, Korea

<sup>e</sup> Heidelberg Institute for Plant Sciences, University of Heidelberg, Heidelberg, Germany

**Rab proteins are members of the Ras superfamily of small GTP binding proteins and play important roles in various intracellular trafficking steps. We investigated the role of Rha1, an Arabidopsis Rab5 homolog, in intracellular trafficking in Arabidopsis protoplasts. In the presence of a dominant-negative mutant of Rha1, soluble vacuolar cargo proteins such as sporamin:green fluorescent protein (Spo:GFP) and Arabidopsis aleurain like protein:GFP are not delivered to the central vacuole; instead, they accumulate as a diffuse or punctate staining pattern within the cell. Spo:GFP at the punctate stains observed in the presence of hemagglutinin:Rha1[S24N] is colocalized with endogenous vacuolar sorting receptor (VSR<sub>At-1</sub>), which is known to localize primarily to the prevacuolar compartment, whereas Spo:GFP in the diffuse pattern is associated with tonoplasts. Furthermore, expression of Rha1[S24N] causes the secretion of a portion of the vacuolar proteins into medium. However, the inhibitory effect of Rha1[S24N] on vacuolar trafficking is relieved partially by coexpressed wild-type Rha1. Based on these results, we propose that Rha1 plays a critical role in the trafficking of soluble cargoes from the prevacuolar compartment to the central vacuole.**

## INTRODUCTION

Proteins of the endomembrane system and secreted proteins are synthesized by ribosomes bound to the endoplasmic reticulum (ER) membrane. These proteins then are transported to their destination from the ER mostly through the Golgi complex (Rothman, 1994; Hawes et al., 1999; Bassham and Raikhel, 2000; Griffiths, 2000). The general pathways taken by the newly synthesized proteins to reach their various destinations have been studied extensively in various organisms and appear to be similar in all eukaryotic organisms examined. The newly synthesized proteins are transported by anterograde trafficking from the ER to their final destinations, such as the vacuole, the plasma membrane, and the extracellular space, by vesicles. Numerous studies in this field show that a large number of proteins are involved in regulating this intracellular traffic (Robinson and Kreis, 1992; Bennett, 1995; Schekman and Orci, 1996; da Silva Conceicao et al., 1997; Stepp et al., 1997; Roth, 1999; Sever et al., 1999; Jin et al., 2001). Furthermore, many different types of lipid molecules also have been shown to play important roles in these processes (Martin, 1997; Corvera et al., 1999; Kim et al., 2001).

Of the proteins involved, many small GTP binding proteins, which are members of the Ras superfamily, have been shown to play important roles at various intracellular trafficking steps (Chavier et al., 1990; Morimoto et al., 1991; Horazdovsky et al., 1994; Pfeffer, 1994; Singer-Kruger et al., 1994; Vadlamudi et al., 2000). Some of these small GTP binding proteins are members of the large Rab subfamily (Pfeffer, 1994; Stenmark et al., 1994; Novick and Zerial, 1997). More than 40 different members of this subfamily have been identified from various organisms and found to be localized at different organelles or to be involved in different intracellular trafficking steps (Chen et al., 1993; Dugan et al., 1995; Zuk and Elferink, 1999; Allan et al., 2000; Batoko et al., 2000). Indeed, it has been suggested that Rab proteins are involved in almost every step of intracellular trafficking (Bucci et al., 1992; Ullrich et al., 1993; Horazdovsky et al., 1994; Feng et al., 1995; Novick and Zerial, 1997; Prekeris et al., 2000; Sonnichsen et al., 2000). One proposed function of Rab family proteins is that they may facilitate the interaction between the v- and t-SNAREs involved in the fusion of vesicles at the target membrane (Rybin et al., 1996; Novick and Zerial, 1997; Waters and Pfeffer, 1999). It also has been suggested that Rab proteins may be involved in generating vesicles at the donor membranes (Prekeris et al., 2000).

In plant cells, many Rab proteins have been identified and characterized at the molecular level (Terry et al., 1993; Borg and Poulsen, 1994; Haizel et al., 1995; Kim et al., 1996). However, the biological roles of these proteins in plant cells usually

<sup>1</sup> To whom correspondence should be addressed. E-mail [ihwang@postech.ac.kr](mailto:ihwang@postech.ac.kr); fax 82-54-279-8159. Article, publication date, and citation information can be found at [www.plantcell.org/cgi/doi/10.1105/tpc.009779](http://www.plantcell.org/cgi/doi/10.1105/tpc.009779).

have been inferred from their amino acid sequence homology with homologs in animal and yeast cells (Terry et al., 1993; Borg and Poulsen, 1994) or by their ability to complement yeast Rab mutants (Kim et al., 1996). Only a few studies have shown directly that these proteins function during intracellular trafficking in plant cells. A tobacco Rab1 homolog has been shown to be involved in anterograde trafficking from the ER to the Golgi apparatus in tobacco cells (Batoko et al., 2000). Ara6 and Ara7 of Arabidopsis, which are homologs of the Rab5 protein in animal cells, have been shown to be localized in Arabidopsis cells at endosomes involved in the endocytosis of FM4-64 (Ueda et al., 2001).

In this study, we investigated the biological role played in intracellular trafficking by Rha1, an Arabidopsis protein that has amino acid sequence homology with Rab5 in animal cells. Here, we present evidence that Rha1 is involved specifically in the trafficking of soluble proteins to the central vacuoles in Arabidopsis protoplasts.

## RESULTS

### Rha1[S24N] Inhibits the Vacuolar Trafficking of Cargo Proteins

A large number of Rab proteins have been identified in plant cells. Among them, Arabidopsis Rha1 (Anuntalabhochai et al., 1991; Terry et al., 1993) is related most closely to the Rab5 protein found in animal cells. To investigate the role of Rha1 in intracellular trafficking, we used the dominant-negative mutant approach using the protoplast-based trafficking assay (Lee et al., 2002). GDP-bound forms of Rabs have been shown to interfere with the activity of the endogenous wild-type protein in a dominant-negative manner by competing for effector proteins (Tisdale et al., 1992; Jones et al., 1998; Li and Liang, 2001).

We selected the vacuolar protein sporamin as the cargo for the intracellular trafficking to the vacuole. Sporamin tagged with green fluorescent protein (Spo:GFP) has been used as a reporter protein for vacuolar trafficking in heterologous systems such as Arabidopsis (Jin et al., 2001; Kim et al., 2001). We first examined the vacuolar trafficking of Spo:GFP (Kim et al., 2001) in the presence of the mutant forms of Rha1 fused with red fluorescent protein (RFP). Cells transformed with *Spo:GFP* alone showed signals either in the central vacuole or in the ER (Figures 1Aa and 1Ab). The GFP signals in the central vacuole (Figure 1Ab) indicate that Spo:GFP was targeted to the central vacuole, whereas the network pattern of GFP signals (Figure 1Aa) suggested Spo:GFP that had not yet been targeted (Jin et al., 2001). With time, the ER pattern (the network pattern) gradually disappeared, whereas the vacuolar pattern increased concomitantly (Figure 1B), indicating that Spo:GFP was transported to the central vacuole with time. Next, we examined the GFP patterns of Spo:GFP in the presence of RFP:Rha1[S24N] (Figure 1A). At 48 h after transformation, the majority of protoplasts showed a diffuse GFP pattern with a few punctate stains (Figures 1Ac to 1Ae; also shown in Figure 1C), and vacuolar patterns were observed rarely. This finding indicates that RFP:Rha1[S24N] may inhibit the targeting of Spo:GFP to the

central vacuole. Expression of RFP:Rha1[S24N] was confirmed by the RFP signals (Figure 1Ad). The RFP signals of RFP:Rha1[S24N] were observed as a diffuse pattern with few punctate stains throughout the time course. To determine the degree of inhibition by Rha1[S24N], we counted the number of protoplasts with the vacuolar GFP pattern from the whole population of protoplasts transformed with *Spo:GFP* and *RFP:Rha1[S24N]* (Figure 1B). When Spo:GFP alone was expressed, its targeting efficiency was 25 and 70% at 24 and 48 h, respectively. However, in the presence of RFP:Rha1[S24N], the targeting efficiency was only 3 and 6% at 24 and 48 h, respectively.

To exclude the possibility that the RFP tag causes this inhibition, we examined the effect on trafficking of Rha1[S24N] tagged with the small epitope hemagglutinin (HA) (Figure 1Ca) and obtained identical results with RFP:Rha1[S24N]. Next, we examined the effect of a dominant-negative mutant of Ara7, which is related closely to Rha1, with 92% amino acid sequence identity. Previously, Ara7 was shown to localize to endosomes (Ueda et al., 2001). In the presence of RFP:Ara7[S24N], Spo:GFP also gave the diffuse pattern with a few punctate stains (Figure 1Cb), suggesting that Ara7 may be functionally equivalent to Rha1 or that transiently expressed RFP:Ara7[S24N] can compete with endogenous Rha1. As controls for the inhibition by RFP:Rha1[S24N], we examined the GFP patterns and targeting efficiency of Spo:GFP in protoplasts expressing RFP:Rha1[T42A] and RFP:Rha1[C198S,C199S]. These two mutants gave diffuse patterns and were present in the cytosol (Figures 1Ag and 1Aj). In the presence of these two mutants, the majority of protoplasts showed the same vacuole patterns observed with Spo:GFP alone (Figures 1Af to 1Ak). In addition, the targeting efficiency of Spo:GFP was not affected by the coexpressed RFP:Rha1[T42A] and RFP:Rha1[C198S,C199S] (Figure 1B). Expression of these mutants in the protoplasts was confirmed by the RFP signals (Figures 1Ag and 1Aj). Thus, Rha1[S24N] acts as a dominant-negative mutant of Rha1 and inhibits the vacuolar trafficking of Spo:GFP to the central vacuole.

To investigate whether Rha1[S24N] also inhibits the trafficking of other vacuolar proteins, we examined the effect of Rha1[S24N] on the trafficking of Arabidopsis aleurain like protein (AALP), a Cys proteinase of Arabidopsis. AALP was shown recently to be targeted to the central vacuole in Arabidopsis cells (Ahmed et al., 2000). We fused AALP to GFP, introduced it into Arabidopsis protoplasts, and examined its GFP patterns (Figure 2A). When AALP:GFP was expressed in protoplasts, even at early time points, the majority of the transformed protoplasts showed the vacuolar GFP patterns, whereas only a minor portion had the network pattern (the ER pattern), indicating that AALP:GFP is transported much more efficiently to the central vacuole than Spo:GFP (cf. Figures 1B and 2B). When *AALP:GFP* was cotransformed with *HA:Rha1[S24N]*, the majority of the protoplasts showed diffuse GFP patterns with few punctate stains rather than vacuolar patterns (Figure 2Ac). The effect of RFP:Rha1[S24N] on the trafficking of AALP:GFP was nearly the same as that of HA:Rha1[S24N]. This finding suggests that Rha1[S24N] also inhibits the trafficking of AALP:GFP to the central vacuole. To confirm this inhibition, we then determined the targeting efficiency of AALP:GFP in the presence of Rha1[S24N] (Figure 2B). The vacuolar trafficking efficiency of

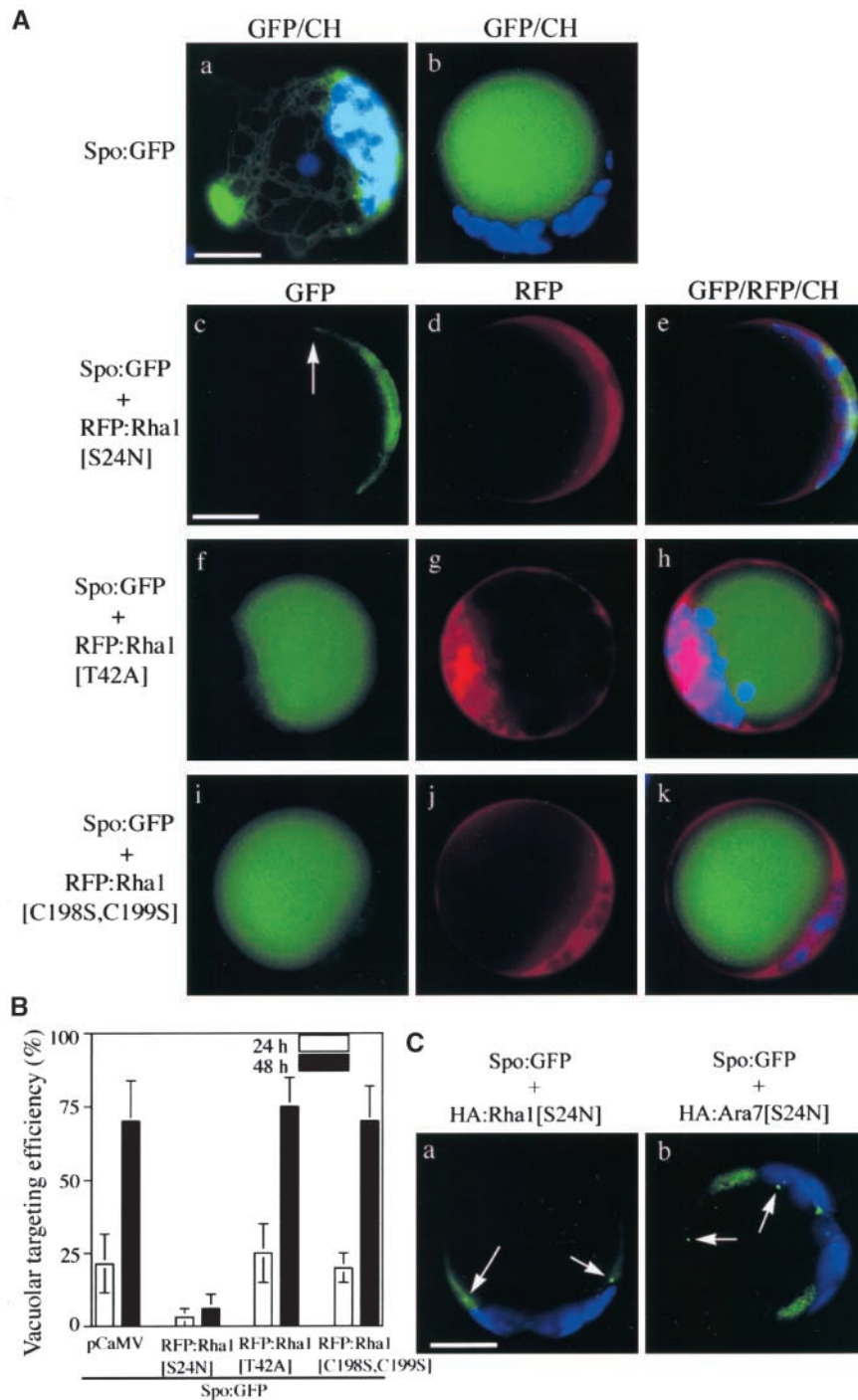


**Figure 1.** Rha1[S24N] Strongly Inhibits the Vacuolar Trafficking of Spo:GFP.

**(A)** GFP patterns of Spo:GFP in the presence of various Rha1 mutants. Protoplasts were transformed with *Spo:GFP* alone or together with *RFP:Rha1[S24N]*, *RFP:Rha1[T42A]*, or *RFP:Rha1[C198S,C199S]*, and the localization of GFP and RFP signals was examined. The GFP patterns shown here are representative of the protoplasts at 48 h after transformation. Blue indicates autofluorescent signals of chlorophyll. The arrow in **(c)** indicates the punctate stain. CH, chloroplasts. Bars = 20  $\mu$ m.

**(B)** Quantification of the degree of inhibition. Protoplasts were transformed with the constructs indicated. *pCaMV* (for *Cauliflower mosaic virus*), a construct identical to *RFP:Rha1* except for the region encoding the RFP:Rha1 fusion protein, was cotransformed with *Spo:GFP* as a balance for transformation and expression. Protoplasts with vacuolar patterns were counted from the whole population of transformed protoplasts at the times indicated. Three independent experiments were performed, and each time image from 50 randomly selected protoplasts was stored. The images were compared carefully based on GFP and chloroplast patterns to exclude the possibility of double scoring the same protoplasts. The patterns finally were scored to estimate the targeting efficiency. The error bars indicate standard deviations.

**(C)** GFP patterns of Spo:GFP in the presence of HA:Rha1[S24N] and HA:Ara7[S24N]. Protoplasts were transformed with the constructs indicated, and the localization of GFP signals was examined at 48 h after transformation. Arrows indicate punctate stains. Bar = 20  $\mu$ m.

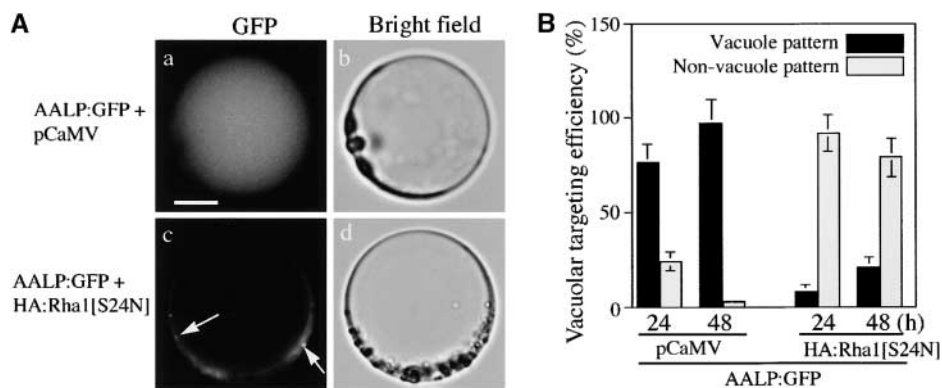


**Figure 2.** Rha1[S24N] Inhibits the Vacuolar Trafficking of AALP:GFP.

**(A)** GFP patterns of AALP:GFP in the presence of HA:Rha1[S24N]. Protoplasts were transformed with the constructs indicated. Localization of AALP:GFP was examined at 24 and 48 h after transformation. Arrows indicate the punctate stains. Bar = 20  $\mu$ m.

**(B)** Quantification of the degree of inhibition. The targeting efficiency was estimated as described in Figure 1B.

AALP:GFP alone was  $\sim$ 96% at 48 h. This was reduced to 21% when HA:Rha1[S24N] was present.

We next examined whether the inhibition of Spo:GFP vacuolar trafficking by Rha1[S24N] is specific to Rha1. Ara6, a plant-specific homolog of Rab5 localized at the endosome, is thought to be involved in endocytosis (Ueda et al., 2001). To determine whether this protein participates in vacuolar trafficking, Ara6[S47N], which has the mutation at the first GTP binding motif, as does Rha1[S24N], was expressed as a HA-tagged form together with Spo:GFP. In the presence of Ara6[S47N]:HA, the GFP patterns of Spo:GFP were similar to those of the control protoplasts (Figure 3A). Furthermore, the vacuolar targeting efficiency of Spo:GFP was not affected in the presence of Ara6[S47N]:HA (Figure 3B). The expression of Ara6[S47N]:HA in protoplasts was examined by protein gel blot analysis with a monoclonal anti-HA antibody. As shown in Figure 3C, the HA antibody detected a protein band at 25 kD, the expected size of Ara6. This finding indicates that Ara6 is not involved in the vacuolar trafficking of cargo proteins.

#### Protein Gel Blot Analysis Confirms the Inhibition of Vacuolar Trafficking by Rha1[S24N]

To confirm that Rha1[S24N] inhibits vacuolar trafficking, we examined the vacuolar trafficking of Spo:GFP and AALP:GFP in greater depth. We first examined the behavior of Spo:GFP over time by protein gel blot analysis (Figure 4A). The GFP antibody detected two bands that were  $\sim$ 30 and 34 kD in size. In addition, the intensity of the 34-kD band was decreased gradually over time, whereas the intensity of the 30-kD band increased concomitantly. Thirty-four kilodaltons was the expected size of Spo:GFP. By contrast, 30 kD was almost the same size as GFP alone. Thus, the lower band may be a proteolytically processed form of Spo:GFP. The gradual increase of the 30-kD band intensity over time is in agreement with such a notion. Often, vacuolar proteins are subjected to partial proteolysis during vacuolar trafficking and/or in the vacuole (Jiang and Rogers, 1998).

Also, GFP targeted to the vacuole has been shown previously to undergo a reduction in molecular mass (Frigerio et al., 2001).

To confirm this possibility, vacuoles were purified from protoplasts by a step-wise Ficoll gradient (Jiang and Rogers, 1998). Protein extracts then were prepared from the purified vacuoles and the nonvacuolar pellet fraction and probed with anti-GFP antibody in protein gel blot analysis (Figure 4B). Only the 30-kD band was detected specifically in the protein extracts obtained from the purified vacuole fraction, whereas the upper band was observed in the protein extracts obtained from the nonvacuolar pellet. In this fractionation method, the prevacuolar compartment (PVC), which is an intermediate compartment between the *trans*-Golgi network and the central (lytic) vacuole in the vacuolar trafficking pathway, is cofractionated with the vacuole (Jiang and Rogers, 1998; Li et al., 2002). To determine whether the vacuolar fraction also contains the PVC, we performed protein gel blot analysis with an anti-vacuolar sorting receptor (VSR) antibody. It has been demonstrated that VSR is concentrated predominantly on the PVCs in fixed root tip cells and tobacco BY-2 suspension culture cells (Li et al., 2002). Thus, an anti-VSR antibody can be used as a marker to define PVCs.

We prepared a polyclonal antibody against VSR<sub>At-1</sub> (anti-VSR), an Arabidopsis BP-80 homolog that is identical to Arabidopsis AtELP (Ahmed et al., 1997). As shown in Figure 4B, VSR<sub>At-1</sub> at 80 kD was detected as both vacuolar and nonvacuolar fractions. Interestingly, VSR<sub>At-1</sub> was distributed nearly equally between the two fractions. The ratio of VSR<sub>At-1</sub> present in the vacuolar and nonvacuolar fractions in Arabidopsis protoplasts was slightly different from that of VSR in tobacco cells. In tobacco cells, 90% of VSR is present in the vacuolar fraction (Li et al., 2002). However, in Arabidopsis cells, AtELP/VSR<sub>At-1</sub> also localizes to the *trans*-Golgi network in addition to the PVC (Sanderfoot et al., 1998; Ahmed et al., 2000). Thus, this result clearly indicates that the PVC is cofractionated with vacuoles. Therefore, we conclude that processed Spo:GFP is either in the PVC and/or within the vacuole. To confirm the fractionation, we detected endogenous aleurain and coexpressed ST:GFP, a

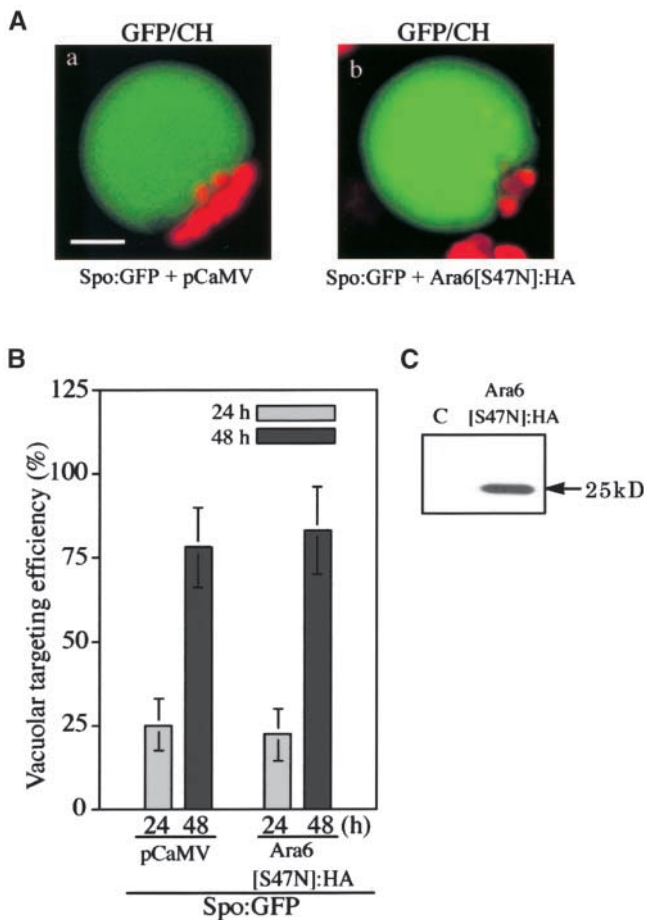


**Figure 3.** Ara6[S47N] Does Not Affect the Vacuolar Trafficking of Spo:GFP.

**(A)** Effect of Ara6[S47N]:HA on vacuolar trafficking. Protoplasts were transformed with *Spo:GFP* plus *pCaMV* or *Spo:GFP* plus *Ara6[S47N]:HA*, and the localization of the GFP signals was examined at 24 and 48 h after transformation. Red indicates autofluorescent signals of chlorophyll. CH, chloroplasts. Bar = 20  $\mu$ m.

**(B)** Quantification of the vacuolar trafficking of Spo:GFP. The targeting efficiency was estimated as described in Figure 1B.

**(C)** Protein gel blot analysis of Ara6[S47N]:HA. Proteins were prepared from transformed protoplasts and analyzed by protein gel blot analysis using a monoclonal anti-HA antibody. C, untransformed protoplasts.

marker for the Golgi apparatus (Lee et al., 2002), as representatives of vacuolar and nonvacuolar proteins, respectively. Endogenous aleurain was detected only in the vacuole fraction and not in the nonvacuolar fraction, whereas ST:GFP was detected only in the nonvacuolar fraction (Figure 4B).

We further investigated the site at which Spo:GFP is processed proteolytically into the 30-kD form by inhibiting the trafficking of Spo:GFP at the ER or the Golgi apparatus. Sar1, a member of the small GTP binding protein family, is involved in the formation of COPII vesicles for anterograde trafficking at the ER (Nakano and Muramatsu, 1989; Yoshihisa et al., 1993). Expression of AtSar1[H74L], a dominant-negative mutant of Arabidopsis Sar1, inhibits anterograde trafficking at the ER

(Takeuchi et al., 2000). AtSar1[H74L] was used to inhibit vacuolar trafficking at the ER, whereas wortmannin and monensin were used to inhibit vacuolar trafficking at the Golgi apparatus (Matsuoka et al., 1995; Kim et al., 2001). Vacuolar trafficking of Spo:GFP was inhibited strongly by AtSar1[H74L] as well as by monensin (Figure 4C). Importantly, the processing of Spo:GFP also was inhibited strongly by the coexpressed AtSar1[H74L] or in the presence of wortmannin and monensin (Figure 4D). These data suggest that the processing occurs downstream of the Golgi apparatus. Thus, as in a previous study (Jiang and Rogers, 1998), Spo:GFP appears to be processed in the PVC and/or within the vacuole.

We next examined the inhibition of vacuolar trafficking by Rha1[S24N] at the protein level (Figure 5A). Protein extracts were prepared at various times and examined by protein gel blot analysis. Spo:GFP still was processed into the 30-kD form in protoplasts expressing HA:Rha1[S24N]. Also, the amount of the 30-kD form was increased with time (Figure 5A). Thus, the processing of Spo:GFP into the 30-kD form per se did not reveal whether HA:Rha1[S24N] inhibits vacuolar trafficking of Spo:GFP to the central vacuole. However, the amount of the 30-kD band present in the two samples was quite different. At 48 h, the amount of the 30-kD band present in the control sample was fourfold higher than that present in the protoplasts expressing HA:Rha1[S24N]. However, unexpectedly, the lower amount of the 30-kD band in the presence of HA:Rha1[S24N] was not accompanied by an increase in the amount of the 34-kD band. The amount of the 34-kD band was only slightly higher in the presence of HA:Rha1[S24N] (Figure 5A).

Often, inhibition or blocking of vacuolar trafficking causes cargo proteins to be secreted into the medium (Matsuoka et al., 1995; Stepp et al., 1997). To examine this possibility, we purified proteins in the culture medium in which the transformed protoplasts were incubated and performed protein gel blot analysis (Figure 5C). A new protein species of  $\sim$ 30.5 kD appeared in the medium when protoplasts were transformed with HA:Rha1[S24N]. The 30.5-kD band intensity increased over time. The 30.5-kD protein species again may be attributable to the proteolytic processing of Spo:GFP by a protease(s) present in the medium. Supporting this notion is the fact that proteins have been shown to be processed proteolytically in the medium after their secretion (Matsuoka et al., 1995; Frigerio et al., 1998). In contrast to Spo:GFP, when GFP was cotransformed with HA:Rha1[S24N], it remained in the cell and was not secreted (Figure 5C). As a positive control for secretion, we examined the GFP-fused *Capsicum annuum* Lipid Transfer Protein1 (CaLTP1), a secreted protein (Park et al., 2002), and found it secreted into the medium as expected. In contrast to HA:Rha1[S24N], Ara6[S47N]:HA did not cause the secretion of Spo:GFP (Figure 5C), indicating that the secretion of Spo:GFP is a specific effect of Rha1[S24N].

To confirm that Rha1[S24N] causes the secretion of vacuolar proteins into the medium in general, we examined whether AALP:GFP also is secreted in the presence of Rha1[S24N]. First, we assessed whether AALP:GFP is processed (Figure 5D). Protoplasts transformed with AALP:GFP had two protein species that could be detected with the GFP antibody, a 70-kD protein and a 30-kD protein. Seventy kilodaltons is the ex-

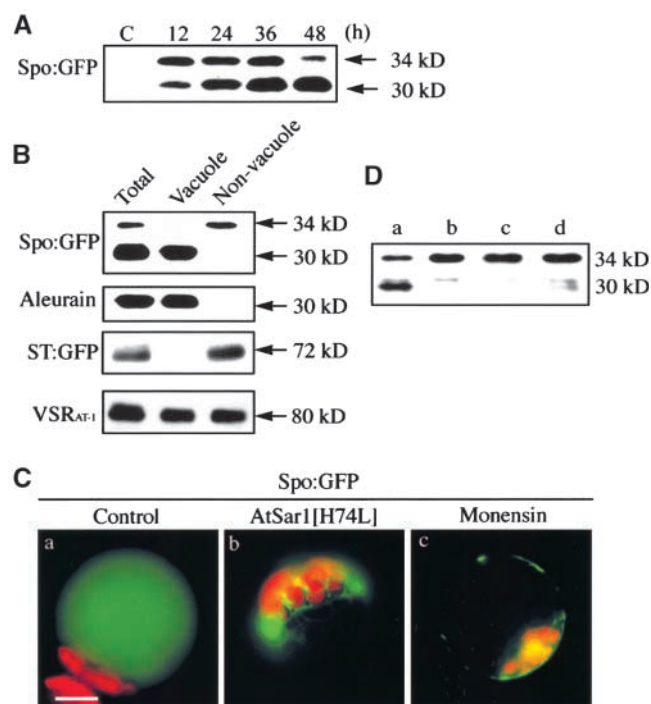


**Figure 4.** Spo:GFP Is Processed Downstream of the Golgi Apparatus during Vacuolar Trafficking.

**(A)** Processing of Spo:GFP. Protein extracts were prepared from protoplasts transformed with *Spo:GFP* at different times after transformation and examined by protein gel blot analysis using anti-GFP antibody. C, untransformed protoplasts.

**(B)** Protein gel blot analysis of vacuolar and nonvacuolar fractions. Protoplasts transformed with *Spo:GFP* and *ST:GFP* were fractionated into vacuolar and nonvacuolar pellet fractions using a Ficoll step gradient. Spo:GFP and ST:GFP present in the vacuolar and nonvacuolar pellet fractions were examined by protein gel blot analysis using an anti-GFP antibody. Endogenous aleurain and endogenous VSR<sub>At-1</sub> also were detected on an identical blot using anti-aleurain and anti-VSR antibodies. Total indicates protein extracts of the protoplasts; vacuole indicates the vacuolar fraction; and non-vacuole indicates the nonvacuolar pellet.

**(C)** GFP patterns of Spo:GFP in the presence of trafficking inhibitors. Protoplasts were transformed with *Spo:GFP* with or without *AtSar1[H74L]*, and the localization of GFP signals was examined 24 to 48 h later. Protoplasts transformed with *Spo:GFP* alone also were treated with monensin (3.5  $\mu$ M) or wortmannin (not shown here, but nearly identical to the pattern shown in [c]) immediately after transformation, and the localization of GFP signals was examined. Red indicates autofluorescent signals of chlorophyll. Bar = 20  $\mu$ m.

**(D)** Protein gel blot analysis of Spo:GFP. Protein extracts were prepared from the protoplasts at 30 h after transformation and examined by protein gel blot analysis. Wortmannin and monensin were added immediately after transformation. Lane a, Spo:GFP alone; lane b, Spo:GFP plus *AtSar1[H74L]*; lane c, Spo:GFP treated with 3.5  $\mu$ M wortmannin; lane d, Spo:GFP treated with 3.5  $\mu$ M monensin.

pected size of AALP:GFP. Thus, the presence of the 30-kD protein indicates that AALP:GFP also is processed proteolytically into a smaller form. Note that the antibody also detected a 65-kD band. This is a cross-reacting endogenous protein (Lee et al., 2001). The 30-kD protein species increased continuously over

time (Figure 5D). In addition, when the protoplasts were fractionated into vacuolar and nonvacuolar fractions by the Ficoll gradient, only the 30-kD protein was present in the vacuoles, whereas the 70-kD band was detected in the nonvacuolar fraction (data not shown), as was Spo:GFP (Figure 4B). In the presence of RFP:Rha1[S24N], the 30-kD band still was detected and its amount increased slightly over time, as observed with Spo:GFP. However, at 36 h, the amount of the 30-kD band was much less than that of the control. In addition, the 70-kD band was secreted into the medium (Figure 5D). The amount of the 70-kD protein in the medium increased over time, indicating that the inhibition of vacuolar trafficking by RFP:Rha1[S24N] causes the secretion of AALP:GFP into the medium, as it does with Spo:GFP. However, unlike Spo:GFP, AALP:GFP in the medium was not processed into a smaller form. The reason for this difference is not understood. Nevertheless, these observations together clearly demonstrate that Rha1[S24N] causes the secretion of the vacuolar proteins Spo:GFP and AALP:GFP into the medium.

#### Coexpressed Wild-Type Rha1 Partially Relieves the Inhibitory Effect of Rha1[S24N] on the Vacuolar Trafficking of Spo:GFP

Next, we examined whether the inhibition caused by RFP Rha1[S24N] can be relieved by coexpressed wild-type Rha1. We reasoned that if the inhibitory effect of Rha1[S24N] is caused by competition between endogenous Rha1 and Rha1[S24N], coexpression of wild-type Rha1 may counteract the inhibitory effect of Rha1[S24N] on vacuolar trafficking. Protoplasts were transformed with *Spo:GFP* and *RFP:Rha1[S24N]* together with varying amounts of *Rha1*. Protein extracts were prepared from protoplasts and incubation medium separately and examined by protein blot analysis using the anti-GFP antibody. As shown in Figure 6A, the amount of Spo:GFP secreted into the medium was reduced significantly in the presence of coexpressed wild-type Rha1. To quantify the degree of inhibition, we first measured the total amount of Spo:GFP. As shown in Figure 6B, the expression level of Spo:GFP in protoplasts was not affected by the presence or absence of wild-type and mutant Rha1[S24N].

To assess the degree of inhibition, we used the amount of Spo:GFP in the incubation medium instead of the amount of proteolytically processed Spo:GFP in protoplasts, because the smaller form is present either in the PVC and/or within the vacuole. As shown in Figure 6B, in the presence of RFP:Rha1[S24N], 14 and 37% of total Spo:GFP was secreted into medium at 24 and 48 h, respectively, after transformation. By contrast, when 10  $\mu$ g of plasmid DNA encoding wild-type Rha1 was cotransformed together with *Spo:GFP* and *RFP:Rha1[S24N]*, 6 and 23% of total Spo:GFP was secreted into medium at 24 and 48 h, respectively, after transformation. When 20  $\mu$ g of wild-type DNA was transformed together with *Spo:GFP* and *RFP:Rha1[S24N]*, the amount of secreted Spo:GFP was reduced further to 4 and 20% at 24 and 48 h, respectively. These results clearly demonstrate that coexpressed wild-type Rha1 partially relieved the inhibitory effect of RFP:Rha1[S24N] on vacuolar trafficking.

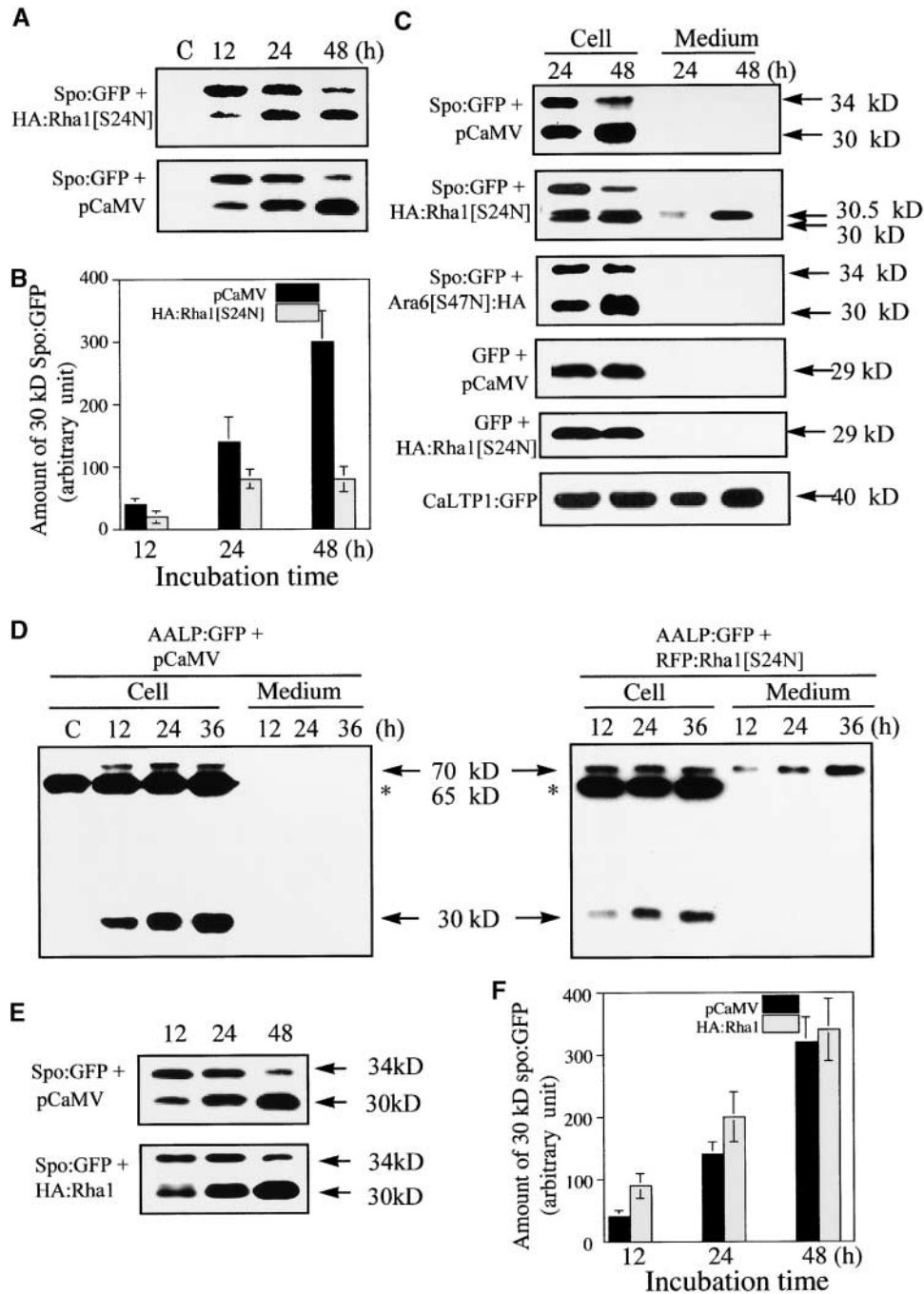


**Figure 5.** Protein Gel Blot Analysis of Spo:GFP and AALP:GFP in the Presence of Rha1[S24N].

**(A)** Protein gel blot analysis of Spo:GFP in the presence of HA:Rha1[S24N]. Protoplasts were transformed with the constructs indicated. Protein extracts were prepared from transformed protoplasts at different times and used for protein gel blot analysis with anti-GFP antibody. pCaMV was used as a balance for transformation and expression. Proteins were prepared from protoplasts and the incubation medium separately. Equal amounts (20  $\mu$ g) of total protein from protoplasts were analyzed by SDS-PAGE. Equal loading of total proteins was confirmed by Coomassie blue staining of protein blots after exposure. C, untransformed protoplasts.

**(B)** Quantification of the processed form of Spo:GFP. The intensity of the 30-kD band was measured at various times using image-analysis software. Identical experiments were performed three times to obtain means and standard deviations.

**(C)** Secretion of Spo:GFP into the medium. Protoplasts were transformed with the constructs indicated. Protein extracts were prepared from protoplasts and the medium at the times indicated and used in protein gel blot analysis with anti-GFP antibody. Equal amounts (20  $\mu$ g) of total protein from protoplasts were analyzed by SDS-PAGE. In the case of protein in the medium, an equal volume was loaded. Equal loading of proteins was confirmed by Coomassie blue staining of protein blots after exposure.

**(D)** Protein gel blot analysis of AALP:GFP in the presence of RFP:Rha1[S24N]. Protoplasts were transformed with the constructs indicated. Protein extracts were prepared from the protoplasts and culture medium and used in protein gel blot analysis. The protein species indicated by asterisks at 65 kD is a cross-reactive endogenous protein species detected by the GFP antibody. Equal amounts (20  $\mu$ g) of total protein from protoplasts were analyzed by SDS-PAGE. In the case of protein in the medium, an equal volume was loaded. Equal loading of proteins was confirmed by Coomassie blue staining of protein blots after exposure.

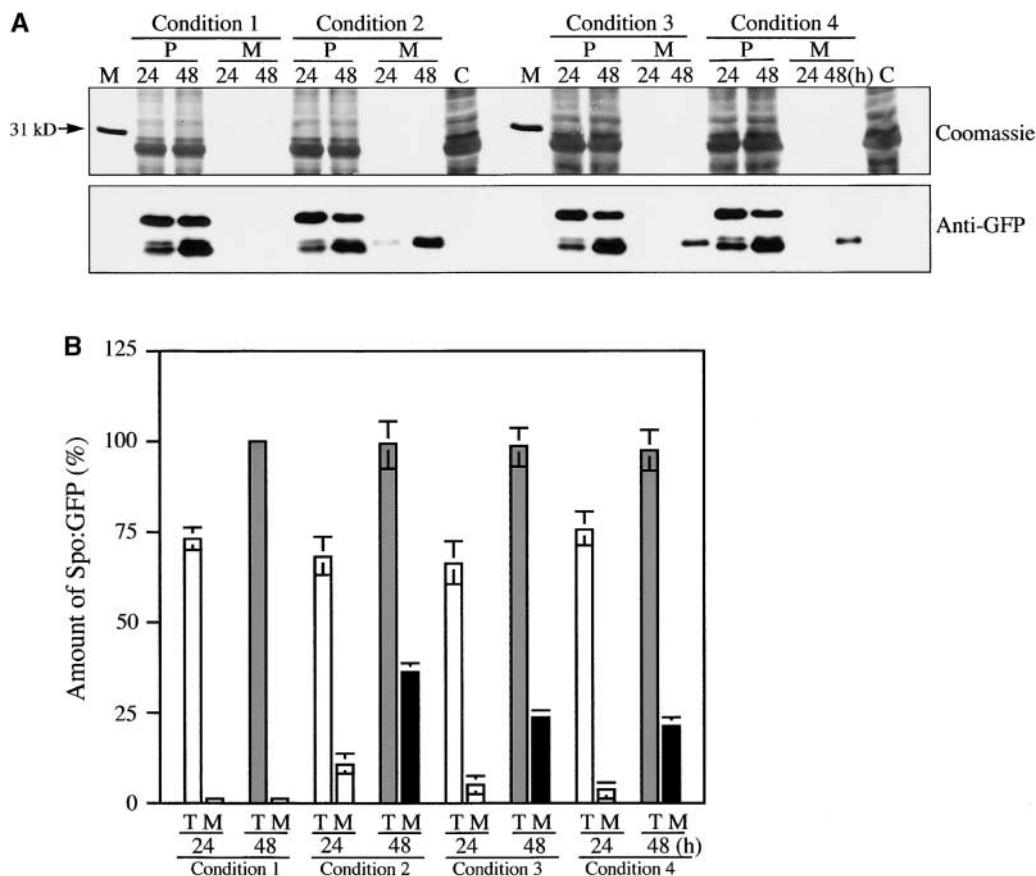


**Figure 6.** Coexpression of Wild-Type Rha1 Partially Releases the Inhibitory Effect of Rha1[S24N] on the Vacuolar Trafficking of Spo:GFP.

**(A)** Protein gel blot analysis of vacuolar trafficking in the presence of coexpressed wild-type Rha1. Protoplasts were transformed with the various constructs indicated. Protoplasts were harvested at 24 and 48 h after transformation. Proteins were prepared from protoplasts and the incubation medium separately. Equal amounts (20  $\mu$ g) of total protein from protoplasts were analyzed by SDS-PAGE. In the case of protein in the medium, an equal volume was loaded. Equal loading of each lane on the gel was confirmed by Coomassie blue staining of the protein blots after exposure. A part of a Coomassie blue-stained blot containing proteins in the range of 25 to 40 kD is shown. Condition 1, Spo:GFP + pCaMV; condition 2, Spo:GFP + RFP:Rha1[S24N] + pCaMV; condition 3, Spo:GFP + RFP:Rha1[S24N] + Rha1 + pCaMV; condition 4, Spo:GFP + RFP:Rha1[S24N] + Rha1. The amount of plasmid DNAs encoding Spo:GFP and RFP:Rha1[S24N] was 5 and 20  $\mu$ g, respectively. For Rha1, 10  $\mu$ g (condition 3) or 20  $\mu$ g (condition 4) of plasmid DNA was used for transformation. The total amount (45  $\mu$ g) of DNA used for transformation was adjusted with pCaMV. Lane M, molecular mass markers; lane C, untransformed protoplasts. M, proteins in medium; P, proteins in protoplasts.

**(B)** Quantification of signal intensities. The intensity of each band was measured using image-analysis software. To compare the degree of inhibition, we determined the percentage of Spo:GFP in the medium from the total amount of Spo:GFP expressed in samples. At least three independent transformation experiments were performed to determine means and standard deviations. Each time, the total amount of Spo:GFP expressed under condition 1 at 48 h was considered 100%. M, proteins in medium; T, total amount of protein present in protoplasts and medium.

### Spo:GFP Accumulates at the PVC or at the Tonoplast of the Central Vacuole in the Presence of Rha1[S24N]

Next, we analyzed the GFP patterns of Spo:GFP and AALP:GFP in the presence of Rha1[S24N] in detail (Figure 7A). Spo:GFP alone yielded two different staining patterns: the ER pattern and the vacuolar pattern (Figures 7Aa and 7Ab). Localization of Spo:GFP in the ER indicates that Spo:GFP is not transported from the ER to the central vacuole (Jin et al., 2001; Kim et al., 2001). However, in the presence of HA:Rha1[S24N], protoplasts showed three different staining patterns: the ER pattern, the punctate staining pattern, and the diffuse pattern (Figures

7Aa, 7Ac, and 7Ad). At 12 and 24 h after transformation, the ER (Figure 7Aa) and punctate (Figure 7Ac) staining patterns predominated, whereas the diffuse pattern (Figure 7Ad) predominated at 48 h. However, at a given time point, the majority of protoplasts had composite patterns, such as the ER pattern plus the punctate staining pattern or the punctate staining pattern together with the diffuse pattern (Figures 1Ac and 1C). When AALP:GFP alone was expressed, nearly all of the transformed protoplasts showed the vacuolar pattern at 48 h after transformation (Figure 7Ae). However, in the presence of Rha1[S24N], AALP:GFP also gave the punctate and/or diffuse patterns (Figures 2Ac, 7Af, and 7Ag), as observed with Spo:GFP.



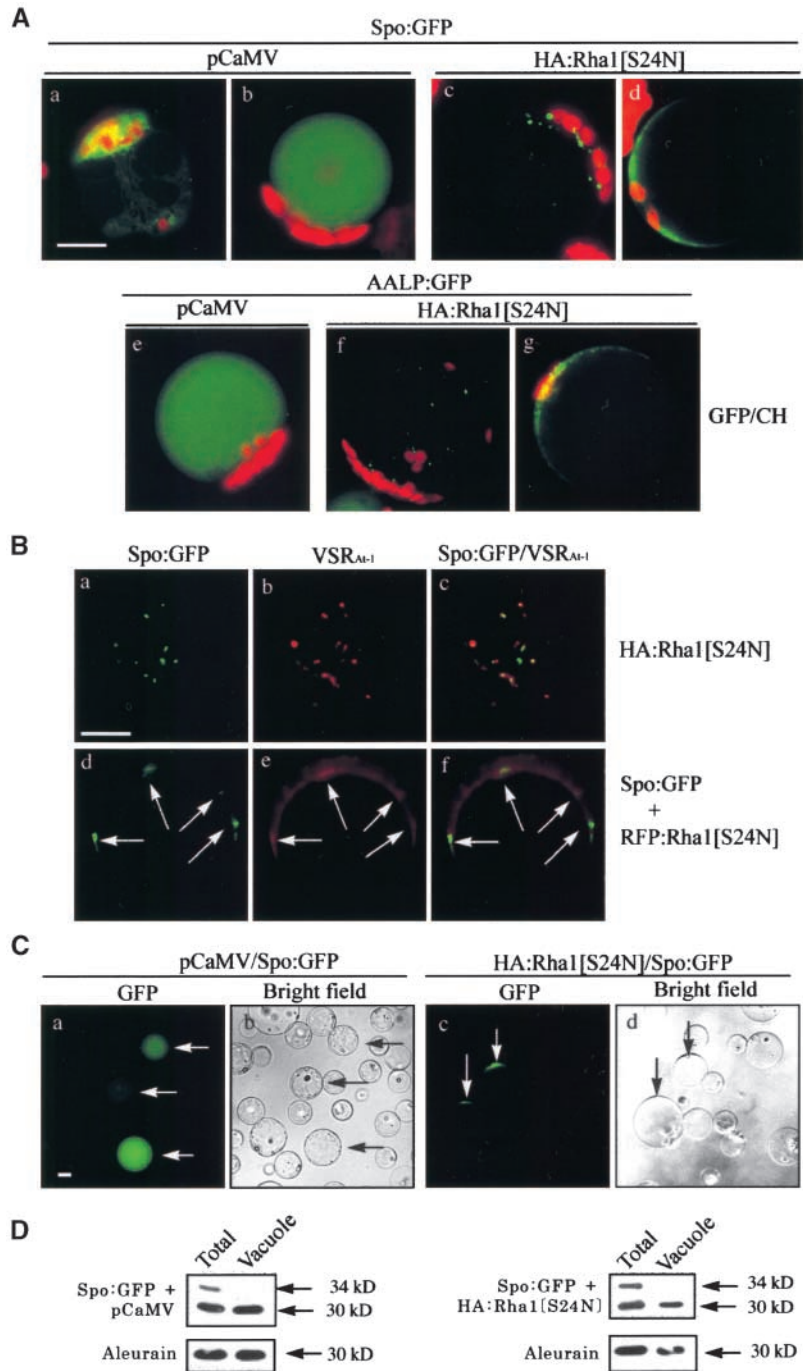


**Figure 7.** Detailed Analysis of GFP Patterns of Reporter Proteins in the Presence of Rha1[S24N].

**(A)** GFP patterns of reporter proteins in the presence of HA:Rha1[S24N]. The localization of the reporter proteins was examined at 24 and 48 h after transformation. Red indicates autofluorescent signals of chlorophyll. CH, chloroplasts. Bar = 20  $\mu$ m.

**(B)** Localization of the punctate stains. Protoplasts were transformed with *Spo:GFP* plus *HA:Rha1[S24N]* (**[a]** to **[c]**) or *Spo:GFP* plus *RFP:Rha1[S24N]* (**[d]** to **[f]**), and the localization of these proteins was examined. To detect the endogenous VSR, protoplasts were fixed with paraformaldehyde and immunostained with anti-VSR antibody (*VSR<sub>At-1</sub>*) followed by Cy3-labeled anti-rat IgG antibody. Also, GFP signals were observed directly from the fixed protoplasts. To quantify the overlap of the green punctate stains with red punctate stains, images of randomly selected transformed protoplasts were captured. From these images of protoplasts, we selected protoplasts that gave clear punctate stains of both *Spo:GFP* and *RFP:Rha1[S24N]* and compared the localization of green and red punctate stains. Arrows in (**[d]** to **[f]**) indicate punctate stains of GFP and RFP signals. Bar = 20  $\mu$ m.

**(C)** Association of GFP signals with the tonoplast membrane. Intact vacuoles were purified from protoplasts transformed with *Spo:GFP* plus *RFP:Rha1[S24N]* or *Spo:GFP* plus *pCaMV* using the Ficoll gradient. The GFP patterns of the purified vacuoles then were examined. Arrows indicate vacuoles with GFP signals. Bar = 20  $\mu$ m.

**(D)** Protein gel blot analysis of *Spo:GFP* copurified with vacuoles. Proteins prepared from the vacuoles were examined by protein gel blot analysis using anti-GFP antibody. Endogenous aleurain was detected with the anti-aleurain antibody. Total indicates unfractionated protein extracts obtained from transformed protoplasts, and vacuole indicates proteins from purified vacuoles.

To better understand the staining patterns, we assessed the localization of the punctate and diffuse patterns of Spo:GFP in the presence of HA:Rha1[S24N]. First, we compared the localization of Spo:GFP at the area of punctate staining with that of endogenous VSR<sub>At-1</sub> at the PVC (Li et al., 2002). As shown in Figure 7B, 90% of the GFP punctate stains had red fluorescent signals of VSR<sub>At-1</sub> detected by the anti-VSR antibody (the number of green punctate stains was 150), indicating that some Spo:GFP may accumulate in the PVC in the presence of HA:Rha1[S24N]. Next, we examined whether transiently expressed RFP:Rha1[S24N] also was detected at the punctate staining compartments observed with Spo:GFP. Protoplasts were cotransformed with Spo:GFP and RFP:Rha1[S24N], and the localization of green and red punctate stains was examined. As shown in Figures 7Be and 7Bf, RFP:Rha1[S24N] was present as a diffuse pattern with a few clear punctate stains. Interestingly, >85% of green punctate stains had red fluorescent signals of RFP:Rha1[S24N] (the number of green punctate stains was 80) (Figures 7Bd and 7Bf, arrows).

Next, we examined the GFP signals in the diffuse pattern, which were localized around the central vacuole. To obtain a clear image of the GFP signals around the central vacuole, the central vacuole was purified from the protoplasts using the Ficoll gradient. Clearly, the GFP signals were present in the purified vacuole (Figure 7Ca) when Spo:GFP alone was expressed. In addition, when vacuoles were purified from the protoplasts coexpressing HA:Rha1[S24N] together with Spo:GFP, the GFP signals were copurified with the central vacuole and present in a crescent pattern at a certain area of the central vacuole but not within the vacuole (Figure 7Cc). Because Spo:GFP is a soluble protein, it cannot be associated with the tonoplast by itself. One possible explanation for our findings is that vesicles or PVCs carrying Spo:GFP may be associated with the tonoplast of the central vacuole but have not yet fused with the tonoplast of the vacuole. To determine the size of Spo:GFP associated with the tonoplast, protein extracts of the purified vacuoles were examined by protein gel blot analysis (Figure 7D). Spo:GFP associated with the tonoplast was the 30-kD form, like the Spo:GFP present within the vacuole. Thus, the processing of Spo:GFP appears to have occurred before the delivery to the central vacuole.

## DISCUSSION

In this study, we used a transient expression system to express various proteins in protoplasts derived from leaf tissues. In a recent review, Sheen (2001) described the successful use of this transient expression system in numerous studies in plants. Despite the advantages of this system, however, the transient expression system also has limitations. A potential problem is that the overexpressed proteins might not faithfully reflect endogenous proteins with respect to subcellular localization and regulation. In particular, an overexpressed protein might be subject to mislocalization and improper regulation, especially if the endogenous protein is present in limiting amounts and tightly controlled. An exogenous protein expressed in protoplasts might behave differently from an endogenous protein in intact plant cells because protoplasts are devoid of cell walls, plas-

modesmata, and cell-cell interactions and are likely to experience various stresses, such as wounding stress. Thus, the results presented here, which were obtained using the transient expression system in protoplasts, should be interpreted with these limitations in mind.

Rha1 shows amino acid sequence homology with Rab5, which plays a critical role in the fusion of endosomes in animals (Li et al., 1994; Sonnichsen et al., 2000). Also, it has 92% amino acid sequence identity to Ara7, which has been shown to localize to endosomes (Ueda et al., 2001). However, the biological function of Rha1 in plants has not been demonstrated directly. To assess this issue, we investigated its role in intracellular trafficking in protoplasts using the dominant-negative mutant approach. From this study, we conclude that Rha1 plays a critical role in the vacuolar trafficking of soluble proteins in Arabidopsis leaf cells. This conclusion is based on the observation that Spo:GFP and AALP:GFP were not transported to the central vacuole in the presence of the dominant-negative mutant but instead accumulated in the cytosol with a diffuse or punctate staining pattern. In addition, protein gel blot analysis showed that vacuolar cargo proteins were secreted into the medium in the presence of the dominant-negative mutant of Rha1.

Rab proteins have been shown to play critical roles in vesicle budding from the donor compartment as well as in vesicle fusion at the target compartment (Chavier et al., 1990; Pfeffer, 1994; Waters and Pfeffer, 1999; Allan et al., 2000; Batoko et al., 2000; Prekeris et al., 2000). Also, Rab proteins have been shown to be involved in the fusion of endosomes or endosomes with lysosomes (Bucci et al., 1992; Pfeffer, 1994; Feng et al., 1995; Rybin et al., 1996; Sonnichsen et al., 2000). In animal and yeast cells, cargo proteins in the late endosomes/PVCs are transported to the lysosomes/vacuoles by fusion. Many Rab proteins are known to be involved in this process (Horazdovsky et al., 1994; Singer-Kruger et al., 1994; Novick and Zerial, 1997; Piper and Luzio, 2001). In plant cells, vacuolar cargo proteins are thought to be transported to the central (or lytic) vacuole through the PVC. As in the case of animal and yeast cells, the endosomes or PVC may fuse to the central vacuole as a means of delivering cargo proteins in plant cells. However, at present, the exact localization of Rha1 is not clear.

When Rha1 was expressed transiently in protoplasts as a GFP- or HA-tagged form, Rha1 gave a punctate staining pattern and colocalized with VSR<sub>At-1</sub> and AtPEP12p (E. Sohn and I. Hwang, unpublished data), raising the possibility that Rha1 also may localize to PVCs. Thus, the Rha1-positive compartments may correspond to the PVC, an intermediate compartment between the *trans*-Golgi network and the central vacuole in the vacuolar trafficking pathway. Supporting this conclusion is the observation that Spo:GFP and RFP:Rha1[S24N] at the punctate stains colocalize with VSR<sub>At-1</sub>. Thus, Rha1 may play a role in the fusion of the PVC to the central vacuole (Figure 8). Then, cargo proteins may remain in the PVC or the PVC may remain associated with the tonoplast but not be able to fuse to the tonoplast in the presence of the dominant-negative Rha1 mutant, as observed. However, at present, in plant cells it is not clear whether cargo proteins are transported from the PVC to the central vacuole by fusion of the PVC to the central vacuole.

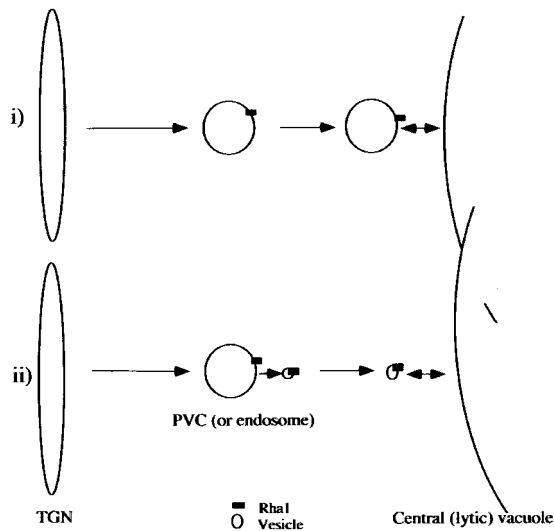


**Figure 8.** Model for the Role of Rha1 in Vacuolar Trafficking.

The observation that Spo:GFP and RFP:Rha1[S24N] at the punctate stains colocalize with VSR<sub>At-1</sub> imply that Rha1 localizes to the PVC. In support of this notion is our preliminary observation that transiently expressed Rha1 in protoplasts gave a punctate staining pattern and colocalized with VSR<sub>At-1</sub> and AtPEP12p, two proteins known to localize to the PVC (E. Sohn and I. Hwang, unpublished data). However, the exact localization of Rha1 needs to be confirmed further. Rha1 could play roles at the PVCs (or endosomes) through its involvement in the fusion of PVCs (or endosomes) or the fusion of endosomes to the central vacuole (i) or in the fusion of vesicles derived from PVCs (or endosomes) to the central vacuole (ii). In the first scenario, we hypothesize that Rha1 recruited to the PVC may be involved directly in the fusion of the PVC to the tonoplast. In the second scenario, we hypothesize that Rha1 recruited to the PVC (or endosome) may be transferred to a vesicle that carries cargo proteins and travel with the vesicle to the tonoplast, where it is involved in the fusion of the vesicle to the tonoplast. TGN, *trans*-Golgi network.

Thus, we cannot exclude the possibility of trafficking of cargo proteins from the PVC to the central vacuole by vesicles (Figure 8). The accumulation of cargo proteins at the PVC or the association of Spo:GFP speckles with the tonoplast can be explained equally by trafficking of vesicles. Inhibition of budding of vesicles at the PVC (or endosomes) may result in the accumulation of cargo proteins at the PVC (or endosomes). Also, in the presence of Rha1[S24N], the vesicles that are somehow tethered at the tonoplast may not be able to fuse to the tonoplast (Waters and Pfeffer, 1999; Allan et al., 2000). To clearly distinguish these two possibilities, it will be necessary to define the nature of the speckles associated with but not fused to the tonoplast in the presence of Rha1[S24N].

Another effect of Rha1[S24N] is that a proportion of the vacuolar proteins was secreted into the medium. This finding suggests that the inhibition of trafficking from the PVC (or endosomes) to the central vacuole may somehow affect the sorting process at the *trans*-Golgi network, which in turn causes some of the vacuolar proteins to be secreted into the medium. Similar secretion of vacuolar proteins has been observed when vacuolar trafficking in plant and yeast cells was inhibited by wort-

mannin or mutations (Matsuoka et al., 1995; Stepp et al., 1997). Although we cannot clearly specify the location where the vacuolar cargoes are diverted from vacuolar trafficking into secretion, we favor the notion that the cargo proteins are secreted from the *trans*-Golgi network. Spo:GFP was processed proteolytically during its transport to the central vacuole from a 34-kD form to a 30-kD form. This event appears to occur downstream of the Golgi apparatus. However, in the presence of Rha1[S24N], Spo:GFP secreted into the medium was found as a 30.5-kD protein. It has been shown that vacuolar cargo proteins secreted into the medium in the presence of wortmannin are processed by a protease present in the medium (Matsuoka et al., 1995; Frigerio et al., 1998). These data together suggest that the full-length Spo:GFP molecule is secreted from the *trans*-Golgi network into the medium, where it is processed into the 30.5-kD form. Supporting this notion is our observation with AALP:GFP. This protein also was degraded from a 70-kD protein to a 30-kD form during its transport to the central vacuole. In the presence of Rha1[S24N], AALP also was secreted into the medium. However, only the 70-kD form was found in the medium.

In animal cells, Rab5 has been shown to be localized to the early endosome and to play a critical role during endocytosis (Li et al., 1994; Rybin et al., 1996; Sonnichsen et al., 2000). By contrast, Rha1, which also gave a punctate staining pattern (E. Sohn and I. Hwang, unpublished data), plays a critical role in vacuolar trafficking. Thus, there is a rather intriguing difference between the roles of Rab5 proteins in animal and plant cells. At present, the difference is not clearly understood. Ara6 is a plant-specific Rab5 protein and is associated with endosomes. The Ara6-positive endosomes are stained with FM4-64 (Ueda et al., 2001). Thus, it is possible that Ara6 may play a role during endocytosis like that of Rab5 in animal cells (Li et al., 1994; Rybin et al., 1996; Sonnichsen et al., 2000). Rha1, on the other hand, may be involved in vacuolar trafficking from the *trans*-Golgi network to the central vacuole. To clearly define the role of Rha1 during vacuolar trafficking, it will be necessary to define the exact localization of Rha1 in plant cells.

## METHODS

### Growth of Plants

*Arabidopsis thaliana* (ecotype Columbia) was grown on Murashige and Skoog (1962) plates in a growth chamber. Leaf tissues were harvested from the plants and used immediately for protoplast isolation.

### Generation of Various Constructs

Rha1 and Ara7 cDNA clones were obtained by PCR from an Arabidopsis cDNA library. The primers were 5'-TCAATCAATCATGGCTAG-3' and 5'-CTAAGCACAACACGATGA-3' for Rha1 and 5'-TCCATGGCTGCA-GCTGGA-3' and 5'-CTAAGCACAACAAGATGA-3' for Ara7. Point mutants of Rha1, Ara7, and Ara6 also were generated by PCR. The primer sets for PCR were as follows: 5'-GATGTTGGAGCTGGAAAAAC-AGTCTTGTGCTACGGTTT-3' and 5'-AAACCGTAGCACAAGACTGTT-TTTCCAGCTCCAACATC-3' for Rha1[S24N], 5'-GTTGAATTTTCAG-GAATCAGCCATTGGTGCAGCCTTTTTC-3' and 5'-GAAAAAGGCTGC-ACCAATGGCTGATTCCTGAAATTC AAC-3' for Rha1[T42A], 5'-TCAATC-

AATCATGGCTAG-3' and 5'-CTAAGCAGAAGACGATGAACTGACTGCGT-3' for Rha1[C198S,C199S], 5'-GATGTTGGTGGCTGGAAAAACAGTCTTGTGTTACGGTTT-3' and 5'-AAACCGTAACACAAGACTGTTTTCACGACCAACATC-3' for Ara7[S24N], and 5'-GACTCTGGTGGTAAATAATTGTATTGTCTTCGATTT-3' and 5'-AAATCGAAGGACAATACAATTTTACCAACACCAGAGTC-3' for Ara6[S47N]. The nucleotide sequences for all of the PCR products were confirmed by nucleotide sequencing. To generate red fluorescent protein (RFP)- or green fluorescent protein (GFP)-tagged Rha1 proteins, RFP- or GFP-coding regions without the termination codon were placed at the N termini of the various Rha1 proteins. To generate hemagglutinin (HA)-tagged Rha1 proteins, pBluescript KS+ (Stratagene) was modified so that it contained the HA tag in the multicloning site. Subsequently, the coding regions of the wild-type and mutant forms of Rha1 were placed downstream of the HA tag. To generate the AALP:GFP fusion construct, the termination codon of AALP was deleted by PCR using two primers, 5'-GAGAAAGCCATGTCTGCGAA-3' and 5'-GGATCCCTGCCGCCACGACAGGGTA-3', and fused to the N-terminus of the GFP-coding region.

### Protein Preparation and Protein Gel Blot Analysis

To prepare cell extracts from protoplasts, transformed protoplasts were lysed by repeated freeze-and-thaw cycles and then centrifuged at 7000g at 4°C for 5 min in a microfuge to remove cell debris (Jin et al., 2001). The proteins present in the medium were prepared by trichloroacetic acid precipitation. Protein gel blot analysis was performed as described previously (Jin et al., 2001).

### Generation of Antibodies

A recombinant protein representing the luminal portion (lacking the transmembrane and cytoplasmic domains) of VSR<sub>At-1</sub> (Paris et al., 1997) was expressed in *Drosophila* S2 cells (Cao et al., 2000). Affinity-purified recombinant protein then was used for the immunization of two rabbits in the animal house at The Chinese University of Hong Kong.

### Purification of the Vacuole from Protoplasts

Protoplast vacuoles were purified according to the method described by Jiang and Rogers (1998). Briefly, transformed protoplasts were loaded onto a Ficoll step gradient consisting of 12 and 15% Ficoll and subjected to ultracentrifugation at 150,000g for 2.5 h. The top and pellet fractions, which contain the intact vacuoles and nonvacuolar endomembrane compartments, respectively, were collected separately from the gradient. The vacuoles were pelleted from the top fraction by centrifugation at 1200g for 5 min. The vacuolar and nonvacuolar endomembrane fractions then were used in protein gel blot analysis.

### Transient Expression and in Vivo Targeting of Reporter Cargo Proteins

The plasmids were introduced by polyethylene glycol-mediated transformation (Jin et al., 2001) into *Arabidopsis* protoplasts that had been prepared from leaf tissues. Expression of the fusion constructs was monitored at various times after transformation, and images were captured with a cooled charge-coupled device camera and a Zeiss (Jena, Germany) Axioplan fluorescence microscope (Jin et al., 2001).

### Immunohistochemistry

Immunohistochemistry with protoplasts was performed as described previously (Frigerio et al., 1998) with slight modifications. Briefly, trans-

formed protoplasts were placed onto poly-L-Lys-coated slides and fixed with 2% paraformaldehyde in a fixing buffer (10 mM Hepes, pH 7.2, 154 mM NaCl, 125 mM CaCl<sub>2</sub>, 2.5 mM maltose, and 5 mM KCl) for 1 h at room temperature. The fixed cells were incubated with rat monoclonal anti-HA or rabbit anti-vacuolar sorting receptor antibodies at 4°C overnight and washed with TSW buffer (10 mM Tris-HCl, pH 7.4, 0.9% NaCl, 0.25% gelatin, 0.02% SDS, and 0.1% Triton X-100) three times. Subsequently, the cells were incubated with Cy3-conjugated goat anti-rabbit IgG (Sigma) or tetramethyl rhodamine isothiocyanate-conjugated anti-rat IgG (Zymed, San Francisco, CA) as the secondary antibodies. The images were captured as described above.

Upon request, all novel materials described in this article will be made available in a timely manner for noncommercial research purposes.

### Accession Numbers

The accession numbers for the proteins described in this article are X59152 (Rha1), AB038491 (Ara7), and AF233883.1 (AALP).

### ACKNOWLEDGMENTS

We thank John Rogers (Washington State University, Pullman) for the anti-aleurain antibody and recombinant VSR<sub>At-1</sub> protein. CaLTP1:GFP was provided by K.H. Paek (Korea University, Seoul, Korea). AtSar1[H74L] and Ara6 were provided by A. Nakano (RIKEN, Wako, Japan). This work was supported by Grant 1ST0222601 from the Creative Research Initiative Program of the Ministry of Science and Technology (Korea). Also, this work was partially supported by grants from the Research Grants Council of Hong Kong (CUHK4156/01M and CUHK4260/02M) to L.J.

Received December 9, 2002; accepted February 27, 2003.

### REFERENCES

- Ahmed, S.U., Bar-Peled, M., and Raikhel, N.V. (1997). Cloning and subcellular location of an Arabidopsis receptor-like protein that shares common features with protein-sorting receptors of eukaryotic cells. *Plant Physiol.* **114**, 325–336.
- Ahmed, S.U., Rojo, E., Kovaleva, V., Venkataraman, S., Dombrowski, J.E., Matsuoka, K., and Raikhel, N.V. (2000). The plant vacuolar sorting receptor AtELP is involved in transport of NH<sub>2</sub>-terminal propeptide-containing vacuolar proteins in *Arabidopsis thaliana*. *J. Cell Biol.* **149**, 1335–1344.
- Allan, B.B., Moyer, B.D., and Balch, W.E. (2000). Rab1 recruitment of p115 into a cis-SNARE complex: Programming budding COPII vesicles for fusion. *Science* **289**, 444–448.
- Anuntalabhojai, S., Terry, N., Van Montagu, M., and Inzé, D. (1991). Molecular characterization of an *Arabidopsis thaliana* cDNA encoding a small GTP-binding protein, Rha1. *Plant J.* **1**, 167–174.
- Bassham, D.C., and Raikhel, N.V. (2000). Unique features of the plant vacuolar sorting machinery. *Curr. Opin. Cell Biol.* **12**, 491–495.
- Batoko, H., Zheng, H.Q., Hawes, C., and Moore, I. (2000). A rab1 GTPase is required for transport between the endoplasmic reticulum and Golgi apparatus and for normal Golgi movement in plants. *Plant Cell* **12**, 2201–2218.
- Bennett, M.K. (1995). SNAREs and the specificity of transport vesicle targeting. *Curr. Opin. Cell Biol.* **7**, 581–586.
- Borg, S., and Poulsen, C. (1994). Molecular analysis of two Ypt/Rab-related sequences isolated from soybean (*Glycine max*) DNA libraries. *Plant Mol. Biol.* **26**, 175–187.

- Bucci, C., Parton, R.G., Mather, I.H., Stunnenberg, H., Simons, K., Hoflack, B., and Zerial, M.** (1992). The small GTPase rab5 functions as a regulatory factor in the early endocytic pathway. *Cell* **70**, 715–728.
- Cao, X., Rogers, S.W., Butler, J., Beevers, L., and Rogers, J.C.** (2000). Structural requirements for ligand binding by a plant vacuolar sorting receptor. *Plant Cell* **12**, 493–506.
- Chavier, P., Parton, R.G., Hauri, H.P., Simons, K., and Zerial, M.** (1990). Localization of low molecular weight GTP binding proteins to exocytic and endocytic compartments. *Cell* **62**, 317–329.
- Chen, Y.T., Holcomb, C., and Moore, H.P.** (1993). Expression and localization of two low molecular weight GTP-binding proteins, Rab8 and Rab10, by epitope tag. *Proc. Natl. Acad. Sci. USA* **90**, 6508–6512.
- Corvera, S., D'Arrigo, A., and Stenmark, H.** (1999). Phosphoinositides in membrane traffic. *Curr. Opin. Cell Biol.* **11**, 460–465.
- da Silva Conceicao, A., Marty-Mazars, D., Bassham, D.C., Sanderfoot, A.A., Marty, F., and Raikhel, N.V.** (1997). The syntaxin homolog AtPEP12p resides on a late post-Golgi compartment in plants. *Plant Cell* **9**, 571–582.
- Dugan, J.M., de Wit, C., McConlogue, L., and Maltese, W.A.** (1995). The Ras-related GTP-binding protein, Rab1B, regulates early steps in exocytic transport and processing of  $\beta$ -amyloid precursor protein. *J. Biol. Chem.* **270**, 10982–10989.
- Feng, Y., Press, B., and Wandinger-Ness, A.** (1995). Rab 7: An important regulator of late endocytic membrane traffic. *J. Cell Biol.* **131**, 1435–1452.
- Frigerio, L., de Virgilio, M., Prada, A., Faoro, F., and Vitale, A.** (1998). Sorting of phaseolin to the vacuole is saturable and requires a short C-terminal peptide. *Plant Cell* **10**, 1031–1042.
- Frigerio, L., Foresti, O., Felipe, D.H., Neuhaus, J.M., and Vitale, A.** (2001). The C-terminal tetrapeptide of phaseolin is sufficient to target green fluorescent protein to the vacuole. *J. Plant Physiol.* **158**, 499–503.
- Griffiths, G.** (2000). Gut thoughts on the Golgi complex. *Traffic* **1**, 738–745.
- Haizel, T., Merkle, T., Turck, F., and Nagy, F.** (1995). Characterization of membrane-bound small GTP-binding proteins from *Nicotiana tabacum*. *Plant Physiol.* **108**, 59–67.
- Hawes, C.R., Brandizzi, F., and Andreeva, A.V.** (1999). Endomembranes and vesicle trafficking. *Curr. Opin. Plant Biol.* **2**, 454–461.
- Horazdovsky, B.F., Busch, G.R., and Emr, S.D.** (1994). VPS21 encodes a rab5-like GTP binding protein that is required for the sorting of yeast vacuolar proteins. *EMBO J.* **13**, 1297–1309.
- Jiang, L., and Rogers, J.C.** (1998). Integral membrane proteins sorting to vacuoles in plant cells: Evidence for two pathways. *J. Cell Biol.* **143**, 1183–1199.
- Jin, J.B., Kim, Y.A., Kim, S.J., Lee, S.H., Kim, D.H., Cheong, G.W., and Hwang, I.** (2001). A new dynamin-like protein, ADL6, is involved in trafficking from the *trans*-Golgi network to the central vacuole in Arabidopsis. *Plant Cell* **13**, 1511–1526.
- Jones, S., Richardson, C.J., Litt, R.J., and Segev, N.** (1998). Identification of regulators for Ypt1 GTPase nucleotide cycling. *Mol. Biol. Cell* **9**, 2819–2837.
- Kim, D.H., Eu, Y.-J., Yoo, C.M., Kim, Y.W., Pih, K.T., Jin, J.B., Kim, S.J., Stenmark, H., and Hwang, I.** (2001). Trafficking of phosphatidylinositol 3-phosphate from the *trans*-Golgi network to the lumen of the central vacuole in plant cells. *Plant Cell* **13**, 287–301.
- Kim, W.Y., Cheong, N.E., Lee, D.C., Lee, K.O., Je, D.Y., Bahk, J.D., Cho, M.J., and Lee, S.Y.** (1996). Isolation of an additional soybean cDNA encoding Ypt/Rab-related small GTP-binding protein and its functional comparison to Sypt using a yeast ypt1-1 mutant. *Plant Mol. Biol.* **31**, 783–792.
- Lee, M.H., Min, M.K., Lee, Y.J., Jin, J.B., Shin, D.H., Kim, D.H., Lee, K.H., and Hwang, I.** (2002). ADP-ribosylation factor 1 of Arabidopsis plays a critical role in intracellular trafficking and maintenance of endoplasmic reticulum morphology in Arabidopsis. *Plant Physiol.* **129**, 1507–1520.
- Lee, Y.J., Kim, D.H., Kim, Y.-W., and Hwang, I.** (2001). Identification of a signal that distinguishes between chloroplast outer envelope membrane and the endomembrane system in vivo. *Plant Cell* **13**, 2175–2190.
- Li, G., Barbieri, M.A., Colombo, M.I., and Stahl, P.D.** (1994). Structural features of the GTP-binding defective Rab5 mutants required for their inhibitory activity on endocytosis. *J. Biol. Chem.* **269**, 14631–14635.
- Li, G., and Liang, Z.** (2001). Phosphate-binding loop and Rab GTPase function: Mutations at Ser29 and Ala30 of Rab5 lead to loss-of-function as well as gain-of-function phenotype. *Biochem. J.* **355**, 681–689.
- Li, Y.B., Rogers, S.W., Tse, Y.C., Lo, S.W., Sun, S.S., Jauh, G.Y., and Jiang, L.** (2002). BP-80 and homologs are concentrated on post-Golgi, probably lytic prevacuolar compartments. *Plant Cell Physiol.* **43**, 726–742.
- Martin, T.F.** (1997). Phosphoinositides as spatial regulators of membrane traffic. *Curr. Opin. Neurobiol.* **7**, 331–338.
- Matsuoka, K., Bassham, D.C., Raikhel, N.V., and Nakamura, K.** (1995). Different sensitivity to wortmannin of two vacuolar sorting signals indicates the presence of distinct sorting machineries in tobacco cells. *J. Cell Biol.* **130**, 1307–1318.
- Morimoto, B.H., Chuang, C.C., and Koshland, D.E., Jr.** (1991). Molecular cloning of a member of a new class of low-molecular-weight GTP-binding proteins. *Genes Dev.* **5**, 2386–2391.
- Murashige, T., and Skoog, F.** (1962). A revised medium for rapid growth and bioassays with tobacco tissue culture. *Physiol. Plant.* **15**, 473–497.
- Nakano, A., and Muramatsu, M.** (1989). A novel GTP-binding protein, Sar1p, is involved in transport from the endoplasmic reticulum to the Golgi apparatus. *J. Cell Biol.* **109**, 2677–2691.
- Novick, P., and Zerial, M.** (1997). The diversity of Rab proteins in vesicle transport. *Curr. Opin. Cell Biol.* **9**, 496–504.
- Paris, N., Rogers, S.W., Jiang, L., Kirsch, T., Beevers, L., Phillips, T.E., and Rogers, J.C.** (1997). Molecular cloning and further characterization of a probable plant vacuolar sorting receptor. *Plant Physiol.* **115**, 29–39.
- Park, C.J., Shin, R., Park, J.M., Lee, G.J., You, J.S., and Paek, K.H.** (2002). Induction of pepper cDNA encoding a lipid transfer protein during the resistance response to tobacco mosaic virus. *Plant Mol. Biol.* **48**, 243–254.
- Pfeffer, S.R.** (1994). Rab GTPases: Master regulators of membrane trafficking. *Curr. Opin. Cell Biol.* **6**, 522–526.
- Piper, R.C., and Luzio, J.P.** (2001). Late endosomes: Sorting and partitioning in multivesicular bodies. *Traffic* **2**, 612–621.
- Prekeris, R., Klumperman, J., and Scheller, R.H.** (2000). A Rab11/Rip11 protein complex regulates apical membrane trafficking via recycling endosomes. *Mol. Cell* **6**, 1437–1448.
- Robinson, M.S., and Kreis, T.E.** (1992). Recruitment of coat proteins onto Golgi membranes in intact and permeabilized cells: Effects of brefeldin A and G protein activators. *Cell* **69**, 129–138.
- Roth, M.G.** (1999). Snapshots of ARF1: Implications for mechanisms of activation and inactivation. *Cell* **97**, 149–152.
- Rothman, J.E.** (1994). Mechanisms of intracellular protein import. *Nature* **372**, 55–63.
- Rybin, V., Ullrich, O., Rubino, M., Alexandrov, K., Simon, I., Seabra, M.C., Goody, R., and Zerial, M.** (1996). GTPase activity of Rab5 acts as a timer for endocytic membrane fusion. *Nature* **383**, 266–269.
- Sanderfoot, A.A., Ahmed, S.U., Marty-Mazars, D., Rapoport, I., Kirchhausen, T., Marty, F., and Raikhel, N.V.** (1998). A putative vacuolar cargo receptor partially colocalizes with AtPEP12p on a prevacuolar compartment in Arabidopsis roots. *Proc. Natl. Acad. Sci. USA* **95**, 9920–9925.

- Schekman, R., and Orci, L.** (1996). Coat proteins and vesicle budding. *Science* **271**, 1526–1533.
- Sever, S., Muhlberg, A.B., and Schmid, S.L.** (1999). Impairment of dynamin's GAP domain stimulates receptor-mediated endocytosis. *Nature* **398**, 481–486.
- Sheen, J.** (2001). Signal transduction in maize and Arabidopsis mesophyll protoplasts. *Plant Physiol.* **127**, 1466–1475.
- Singer-Kruger, B., Stenmark, H., Dusterhoft, A., Philippsen, P., Yoo, J.S., Gallwitz, D., and Zerial, M.** (1994). Role of three rab5-like GTPases, Ypt51p, Ypt52p, and Ypt53p, in the endocytic and vacuolar protein sorting pathways of yeast. *J. Cell Biol.* **125**, 283–298.
- Sonnichsen, B., De Renzis, S., Nielsen, E., Rietdorf, J., and Zerial, M.** (2000). Distinct membrane domains on endosomes in the recycling pathway visualized by multicolor imaging of Rab4, Rab5, and Rab11. *J. Cell Biol.* **149**, 901–914.
- Stenmark, H., Valencia, A., Martinez, O., Ullrich, O., Goud, B., and Zerial, M.** (1994). Distinct structural elements of rab5 define its functional specificity. *EMBO J.* **13**, 575–583.
- Stepp, J.D., Huang, K., and Lemmon, S.K.** (1997). The yeast adaptor protein complex, AP-3, is essential for the efficient delivery of alkaline phosphatase by the alternate pathway to the vacuole. *J. Cell Biol.* **139**, 1761–1774.
- Takeuchi, M., Ueda, T., Sato, K., Abe, H., Nagata, T., and Nakano, A.** (2000). A dominant negative mutant of sar1 GTPase inhibits protein transport from the endoplasmic reticulum to the Golgi apparatus in tobacco and Arabidopsis cultured cells. *Plant J.* **23**, 517–525.
- Terryn, N., Arias, M.B., Engler, G., Tire, C., Villarroel, R., Van Montagu, M., and Inzé, D.** (1993). rha1, a gene encoding a small GTP binding protein from Arabidopsis, is expressed primarily in developing guard cells. *Plant Cell* **5**, 1761–1769.
- Tisdale, E.J., Bourne, J.R., Khosravi-Far, R., Der, C.J., and Balch, W.E.** (1992). GTP-binding mutants of rab1 and rab2 are potent inhibitors of vesicular transport from the endoplasmic reticulum to the Golgi complex. *J. Cell Biol.* **119**, 749–761.
- Ueda, T., Yamaguchi, M., Uchimiya, H., and Nakano, A.** (2001). Ara6, a plant-unique novel type Rab GTPase, functions in the endocytic pathway of *Arabidopsis thaliana*. *EMBO J.* **20**, 4730–4741.
- Ullrich, O., Stenmark, H., Alexandrov, K., Huber, L.A., Kaibuchi, K., Sasaki, T., Takai, Y., and Zerial, M.** (1993). Rab GDP dissociation inhibitor as a general regulator for the membrane association of rab proteins. *J. Biol. Chem.* **268**, 18143–18150.
- Vadlamudi, R.K., Wang, R.A., Talukder, A.H., Adam, L., Johnson, R., and Kumar, R.** (2000). Evidence of Rab3A expression, regulation of vesicle trafficking, and cellular secretion in response to heregulin in mammary epithelial cells. *Mol. Cell. Biol.* **20**, 9092–9101.
- Waters, M.G., and Pfeffer, S.R.** (1999). Membrane tethering in intracellular transport. *Curr. Opin. Cell Biol.* **11**, 453–459.
- Yoshihisa, T., Barlowe, C., and Schekman, R.** (1993). Requirement for a GTPase-activating protein in vesicle budding from the endoplasmic reticulum. *Science* **259**, 1466–1468.
- Zuk, P.A., and Elferink, L.A.** (1999). Rab15 mediates an early endocytic event in Chinese hamster ovary cells. *J. Biol. Chem.* **274**, 22303–22312.

**Rha1, an Arabidopsis Rab5 Homolog, Plays a Critical Role in the Vacuolar Trafficking of Soluble Cargo Proteins**

Eun Ju Sohn, Eol Sun Kim, Min Zhao, Soo Jin Kim, Hyeran Kim, Yong-Woo Kim, Yong Jik Lee, Stefan Hillmer, Uik Sohn, Liwen Jiang and Inhwan Hwang

*Plant Cell* 2003;15;1057-1070; originally published online April 3, 2003;

DOI 10.1105/tpc.009779

This information is current as of December 5, 2020

<b>References</b>	This article cites 64 articles, 35 of which can be accessed free at: <a href="/content/15/5/1057.full.html#ref-list-1">/content/15/5/1057.full.html#ref-list-1</a>
<b>Permissions</b>	<a href="https://www.copyright.com/ccc/openurl.do?sid=pd_hw1532298X&amp;issn=1532298X&amp;WT.mc_id=pd_hw1532298X">https://www.copyright.com/ccc/openurl.do?sid=pd_hw1532298X&amp;issn=1532298X&amp;WT.mc_id=pd_hw1532298X</a>
<b>eTOCs</b>	Sign up for eTOCs at: <a href="http://www.plantcell.org/cgi/alerts/ctmain">http://www.plantcell.org/cgi/alerts/ctmain</a>
<b>CiteTrack Alerts</b>	Sign up for CiteTrack Alerts at: <a href="http://www.plantcell.org/cgi/alerts/ctmain">http://www.plantcell.org/cgi/alerts/ctmain</a>
<b>Subscription Information</b>	Subscription Information for <i>The Plant Cell</i> and <i>Plant Physiology</i> is available at: <a href="http://www.aspb.org/publications/subscriptions.cfm">http://www.aspb.org/publications/subscriptions.cfm</a>